JOURNAL OF VIROLOGY, Mar. 2010, p. 2212–2222 Vol. 84, No. 5
0022-538X/10/$12.00 doi:10.1128/JVI.01388-09

ICP27 Phosphorylation Site Mutants Display Altered Functional Interactions with Cellular Export Factors Aly/REF and TAP/NXF1 but Are Able To Bind Herpes Simplex Virus 1 RNA▽

Kara A. Corbin-Lickfett,[1]§ Santos Rojas,[1]§ Ling Li,[1]† Melanie J. Cocco,[2] and Rozanne M. Sandri-Goldin[1]*

Departments of Microbiology and Molecular Genetics[1] and Molecular Biology and Biochemistry,[2] University of California, Irvine, California 92697

Received 6 July 2009/Accepted 7 December 2009

Herpes simplex virus 1 (HSV-1) protein ICP27 is a multifunctional regulatory protein that is phosphorylated. Phosphorylation can affect protein localization, protein interactions, and protein function. The major sites of ICP27 that are phosphorylated are serine residues 16 and 18, within a CK2 site adjacent to a leucine-rich region required for ICP27 export, and serine 114, within a PKA site in the nuclear localization signal. Viral mutants bearing serine-to-alanine or glutamic acid substitutions at these sites are defective in viral replication and gene expression. To determine which interactions of ICP27 are impaired, we analyzed the subcellular localization of ICP27 and its colocalization with cellular RNA export factors Aly/REF and TAP/NXF1. In cells infected with phosphorylation site mutants, ICP27 was confined to the nucleus even at very late times after infection. ICP27 did not colocalize with Aly/REF or TAP/NXF1, and overexpression of TAP/NXF1 did not promote the export of ICP27 to the cytoplasm. However, *in vitro* binding experiments showed that mutant ICP27 was able to bind to the same RNA substrates as the wild type. Nuclear magnetic resonance (NMR) analysis of the N terminus of ICP27 from amino acids 1 to 160, compared to mutants with triple substitutions to alanine or glutamic acid, showed that the mutations affected the overall conformation of the N terminus, such that mutant ICP27 was more flexible and unfolded. These results indicate that these changes in the structure of ICP27 altered *in vivo* protein interactions that occur in the N terminus but did not prevent RNA binding.

ICP27 is a multifunctional protein that acts at both the transcriptional and posttranscriptional levels (47). At the transcriptional level, ICP27 interacts with the C-terminal domain (CTD) of RNA polymerase II (RNAP II) and recruits RNAP II to sites of herpes simplex virus 1 (HSV-1) transcription/replication (13, 59). The interaction of ICP27 with RNAP II requires the N-terminal leucine-rich region (LRR) of ICP27, and the viral mutant dLeu, in which this region is deleted, cannot interact with and recruit RNAP II (13). As a result, viral early and late transcript levels are reduced to 10 to 20% of the levels seen in wild-type HSV-1 infection (32). At the posttranscriptional level, ICP27 interacts with SR proteins, which are essential splicing factors, and with SRPK1, an SR protein-specific kinase, to mediate the aberrant phosphorylation of SR proteins (50). Inappropriately phosphorylated SR proteins are unable to participate in spliceosome assembly, and host cell pre-mRNA splicing is inhibited (19, 50), which contributes to the shutoff of host protein synthesis (18). Beginning about 5 h after infection, ICP27 leaves splicing speckles and recruits the cellular mRNA export factor Aly/REF to viral transcription/replication sites (8, 9). ICP27 then binds viral RNAs (46) and begins shuttling between the nucleus and cytoplasm in its role as an RNA export factor (8, 9, 28, 39, 46, 52). ICP27 is exported to the cytoplasm through the TAP/NXF1 mRNA export pathway, and the interaction with TAP/NXF1 requires the N-terminal LRR. ICP27 mutants with lesions in the LRR are confined to the nucleus, and viral RNA export to the cytoplasm is severely reduced (23, 24).

ICP27 is modified posttranslationally by phosphorylation and arginine methylation (38, 53, 58). Both modifications have been shown to affect protein-protein interactions and protein-nucleic acid interactions and to modulate import and export of proteins (2, 22). Interestingly, both modifications occur in the N terminus of ICP27. The major sites of arginine methylation determined by mass spectrometry are within an RGG box motif at arginine residues 138, 148, and 150 (53). The major sites of ICP27 phosphorylation determined by phosphopeptide mapping studies (58) are on serine residues 16 and 18 within a consensus CK2 site, adjacent to the LRR, and on serine residue 114 within a PKA site in the nuclear localization signal (NLS). We investigated the role that arginine methylation plays in regulating ICP27 export and protein interactions (53, 54). Viral mutants in which the arginine residues in the RGG box were substituted with lysine were constructed. During infection with these mutants, ICP27 was exported to the cytoplasm earlier and more rapidly than the wild-type ICP27 (53). In addition, the functional interactions of ICP27 with SRPK1, which interacts with ICP27 through the RGG box (50), and

* Corresponding author. Mailing addresss: Department of Microbiology and Molecular Genetics, School of Medicine, Medical Sciences I, Rm. B240, University of California at Irvine, Irvine, CA 92697-4025. Phone: (949) 824-7570. Fax: (949) 824-9054. E-mail: rmsandri@uci.edu.

§ Both authors contributed equally to this work.

† Present address: Verdezyne, Inc., Carlsbad, CA.

▽ Published ahead of print on 16 December 2009.

Aly/REF, which interacts with ICP27 through a region that spans the NLS and RGG box (9), were impaired in infections with the substitution mutants (54). These findings indicate that ICP27 export and functional interactions with two cellular proteins are modulated by arginine methylation.

To determine the role that phosphorylation plays in regulating the subcellular localization and protein interactions of ICP27, we constructed viral mutants bearing single, double, and triple substitutions of alanine or glutamic acid for serine residues at positions 16, 18, and 114. Characterization of these mutants revealed that virus yields were reduced by two logs or more, and DNA replication and expression of early and late gene products were greatly decreased (45). In infections with the phosphorylation site mutants, ICP4-containing replication compartment formation was severely curtailed. Further, ICP27 did not colocalize with RNAP II. The interaction of the CTD of RNAP II with ICP27 requires the LRR (13), and serines 16 and 18 are adjacent to the LRR, which suggests that phosphorylation may modulate ICP27's interaction with RNAP II. The goal of this study was to further define which activities and functional interactions of ICP27 are regulated by phosphorylation. To this end, we analyzed the subcellular localization of ICP27 in cells infected with the phosphorylation site mutants and investigated the functional interaction of mutant ICP27 with Aly/REF and TAP/NXF1, which interact with ICP27 through regions spanning the NLS and LRR, respectively.

MATERIALS AND METHODS

Cells, viruses, and recombinant plasmids. HeLa cells were grown in minimal essential media (MEM) with 10% newborn calf serum. Vero cells were grown in MEM with 8% fetal bovine serum and 4% donor calf serum at 37°C. HSV-1 KOS and 27-LacZ were previously described (51). The ICP27 phosphorylation site viral mutants S16A; S18A; S114A; S16,18A; S16,18,114A; S16E; S18E; S16,18E; and S16,18,114E were constructed and characterized as described previously (45). ICP27 mutant viruses dLeu, d2-3, and d3-4 were described previously (8, 31) and were kindly provided by Steve Rice (University of Minnesota). Plasmid pEGFP-Aly/REF has been described previously (9). Plasmid pEGFP-TAP was generously provided by E. Izaurralde (1). The codon-optimized ICP27 gene was obtained from Verdezyne, Inc. (formerly CODA Genomics) and has been described (10). PCR was used to amplify the sequences corresponding to the 160 ICP27 N-terminal amino acids, and this sequence was cloned into the NdeI and XhoI sites of plasmid pET21b (Novagen) with a C-terminal His tag. The S16,18,14A and S16,18,114E ICP27 N-terminal mutants were constructed using a QuickChange site-directed mutagenesis kit (Stratagene). Two rounds of mutagenesis were performed to construct each triple mutant. The wild-type pET21b-ICP27 N terminus was used as the template for mutagenesis. The first round of mutagenesis for S16,18,114A used the forward primer 5′-CTGGGTC TGGACCTGGCTGACGCTGACCTGGACGAAG-3′ and reverse primer 5′-C TTCGTCCAGGTCAGCGTCAGCCAGGTCCAGACCCAG-3′, changing serines 16 and 18 to alanine. The second round of mutagenesis used the forward primer 5′-GTGCTCGCCGTCCGGCTTGCTCTCCAGAACG-3′ and the reverse primer 5′-CGTTCTGGAGAGCAAGCCGGACGGCGAGCAC-3′, changing serine 114 to alanine. The first round of mutagenesis for S16,18,114E used the forward primer 5′-CTGGGTCTGGACCTGGAAGACGAAGACCTGGACGAAG-3′ and reverse primer 5′-CTTCGTCCAGGTGTTCGTGTTCCAGGTCCAGACC CAG-3′, changing serines 16 and 18 to glutamic acid. The second round of mutagenesis used the forward primer 5′-GTGCTCGCCGTCCGGAATGCTCT CCAGAACG-3′ and the reverse primer 5′-CGTTCTGGAGAGCATTCCGGA CGGCGAGCAC-3′, changing serine 114 to glutamic acid.

Immunofluorescence microscopy. HeLa cells were seeded on coverslips in 24-well dishes and were transfected 12 h later with either pEGFP-Aly/REF or pEGFP-TAP, using Lipofectamine 2000 reagent (Invitrogen) as described in the manufacturer's protocol. Twenty-four hours after transfection, cells transfected with pEGP-Aly/REF were infected with HSV-1 KOS, S16E, S16,18,114E, or d2-3 at a multiplicity of infection (MOI) of 5 (see Fig. 3). Cells transfected with pEGFP-TAP were infected with KOS, S16E, or S16,18,114E at an MOI of 5 (see Fig. 5). Cells were fixed with 3.7% formaldehyde at the times indicated in the legends for Fig. 1, 2, 3, and 5. Immunofluorescent staining was performed with ICP27-specific monoclonal antibody P1119 (Virusys) as previously described (8, 9). GFP-Aly/REF and GFP-TAP/NXF1 fluorescence was visualized directly. Double staining for SC35 and ICP27 was performed as previously described, using P1119, anti-SC35 hybridoma supernatant (50), and Texas Red dye-conjugated AffiniPure goat anti-mouse IgG (Jackson ImmunoResearch) as the secondary antibody (1:300). Cells were viewed with a Zeiss Axiovert S100 microscope at a magnification of ×100 or an LSM 510 confocal microscope at a magnification of ×63. Images were analyzed with Adobe Photoshop, the LSM 510 image browser, and AxioVision 4.7.

Immunoprecipitation. HeLa cells were either mock infected or were infected with wild-type KOS or S16,18,114A at an MOI of 5. Eight hours after infection, cells were harvested, and immunoprecipitation was performed on cell lysates using anti-ICP27 antibodies P1119 and P1113 (Virusys) as described previously (9). Immunoprecipitated complexes were fractionated by SDS-polyacrylamide gel electrophoresis and transferred to nitrocellulose. Western blot analysis was performed as described previously (54) with anti-ICP27 antibodies and anti-Aly/REF antibody (Sigma).

Complementation assay. HeLa cells were infected singly with KOS, S16A, S16E, S114A, S114E, S16,18,114A, or S16,18,114E at an MOI of 5. In coinfections, each virus was added at an MOI of 2.5 (see Fig. 6). Samples were harvested at 24 h after infection. Plaque assays were performed on 2-2 cells to determine viral titers.

Protein expression and purification. pET21b plasmids expressing the 160 N-terminal amino acids of wild-type, codon-optimized, His-tagged ICP27, the triple serine-to-alanine mutant, S16,18,114A, or the triple serine-to-glutamic acid mutant, S16,18,114E were transformed into *Escherichia coli* strain BL21 Rosetta (Novagen). Cultures were grown in Luria Bertani (LB) broth with 50 μg/ml ampicillin for protein to be used in electrophoretic mobility shift assays (EMSA) or Neidhart's minimal media supplemented with 15 mM $^{15}NH_4Cl$ and containing 50 μg/ml ampicillin for NMR analysis. Cultures were grown to an optical density at 600 nm (OD_{600}) of 0.8 to 1.0 and were induced with 100 μM IPTG (isopropyl-β-D-thiogalactopyranoside) (Sigma) for 3 h at 37°C. His-tagged ICP27 proteins were purified using nickel nitrilotriacetic acid (Ni-NTA) agarose (Qiagen) according to the manufacturer's recommendation for native protein purification. ICP27 N-terminal proteins were dialyzed into 50 mM Tris buffer, pH 8, for EMSA or NMR buffer (50 mM Na_2HPO_4, 50 mM NaH_2PO_4, 100 mM NaCl, and 200 mM K_2S0_4, pH 8.0) for NMR analysis, and samples were concentrated with a Centriprep centrifugal filter device (Millipore). The Coomassie Plus Bradford assay kit (Pierce) was used to determine protein concentration.

Electrophoretic mobility shift assay. Oligonucleotide sequences from the glycoprotein C gene (gC), which were described previously (10), were used in the EMSAs. Five picomoles of the following were added: gC 1–30 (5′-CGCCGAC CCTCCGTTGTATTCTGCACCGG-3′), gC 11–40 (5′-CCGTTGTATTCTGTC ACCGGGCCGCTGCCG-3′), and gC 31–60 (5′-GCCGCTGCCGACCCAGCG GCTGATTATCGG-3′). The oligonucleotides were radiolabeled with [γ-^{32}P] ATP with Optikinase (USB) and purified using the Qiaquick nucleotide removal kit (Qiagen). Twenty femptomoles of each oligonucleotide was incubated with 2.5 to 62.5 μM wild-type ICP27 N-terminal peptide, S16,18,114A, or S16,18,114E in 1× binding buffer (20 mM Tris, pH 8; 150 mM KCl; 1 mM EDTA, pH 8; and 1 mM dithiothreitol [DTT]) with 10% glycerol and 300 μg/ml bovine serum albumin (BSA) for 30 min at 37°C. Samples were loaded onto prerun 5% acrylamide/bisacrylamide gels with 2.5% (wt/vol) glycerol and 1× Tris acetate buffer and subjected to electrophoresis for 2 h at 35 mA. Gels were vacuum dried onto filter paper and exposed to film.

NMR analysis. NMR protein samples were prepared in 50 mM Na_2HPO_4, 50 mM NaH_2PO_4, 100 mM NaCl, 200 mM K_2S0_4 (pH 8), and 10% D_20 at a final concentration of 0.3 mM. NMR spectra were recorded on a Varian 800-MHz spectrometer at 25°C. The ^{1}H-^{15}N heteronuclear single quantum coherence (HSQC) pulse sequence (27) was used for characterization of the wild-type and mutant ICP27 N-terminal peptides. Data were processed with NMRpipe (14). Wild-type ICP27 N-terminal HSQC spectra were 1,024 points (^{1}H) and 72 points (^{15}N); S16,18,114A and S16,18,114E mutant HSQC spectra were 1,024 points (^{1}H) and 60 points (^{15}N). All spectra were processed with shifted sine function and zero filled to twice the size in each dimension.

RESULTS

ICP27 is sequestered in the nucleus during infection with phosphorylation site mutants. In wild-type HSV-1-infected cells, ICP27 is predominantly nuclear at early times, but it

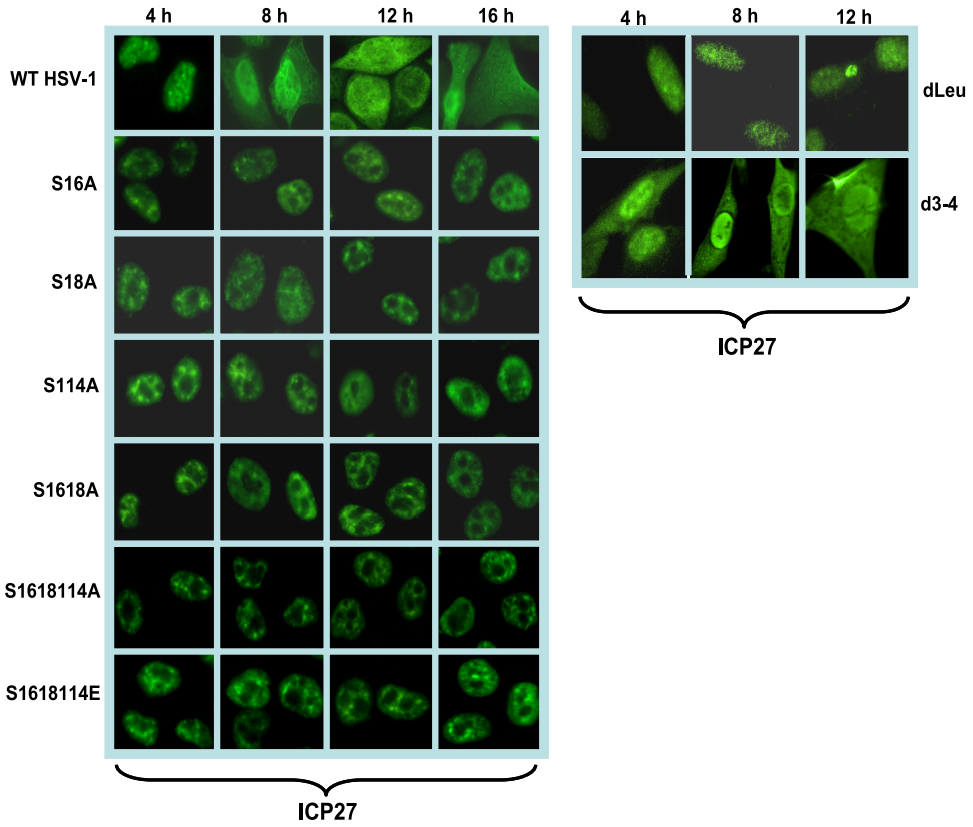

FIG. 1. ICP27 is confined to the nucleus in infection with phosphorylation site mutants. HeLa cells were infected with HSV-1 KOS, S16A, S18A, S114A, S16,18A, S16,18,114A, S16,18,114E, dLeu, and d3-4 at an MOI of 5. At 4, 8, 12, and 16 h postinfection, cells were fixed with 3.7% formaldehyde and immunostained with anti-ICP27 monoclonal antibody. Cells were viewed with a Zeiss Axiovert S100 microscope. Magnification, ×100.

shuttles between the nucleus and cytoplasm beginning about 5 h after infection (8, 9, 23, 28, 46, 52). Phosphorylation has been shown to affect protein import into the nucleus and protein export to the cytoplasm (4, 15, 17, 22, 26, 57). Therefore, we examined the localization of ICP27 in infections with the phosphorylation site mutants. The major NLS of ICP27 has been mapped to amino acids 110 to 137 (37), and the RGG box from residues 138 to 152 also contributes to the efficiency of ICP27 import (20). Serine 114 maps within the NLS, and therefore, phosphorylation at this site may regulate protein import. Cells infected with wild-type KOS and the phosphorylation site mutants S16A, S18A, S114A, S16,18A, S16,18,114A, and S16,18,114E were analyzed by immunofluorescent staining of ICP27 at the times indicated in Fig. 1. Cells were also infected with mutant d3-4 in which the NLS from residues 109 to 138 are deleted (37). In wild-type KOS-infected cells, ICP27 was nuclear at 4 h after infection and was seen in both the nucleus and cytoplasm at 8, 12, and 16 h after infection, when it was actively shuttling between the nucleus and cytoplasm (Fig. 1). In contrast, in mutant d3-4-infected cells, ICP27 in both the nucleus and cytoplasm was seen, even at 4 h after infection, indicating inefficient import into the nucleus (Fig. 1). In the phosphorylation site mutant-infected cells, ICP27 was exclusively nuclear at all times analyzed. This result indicates that nuclear import of ICP27 is not impaired in the phosphorylation site mutant-infected cells. This result also indicates that export was impaired because ICP27 was not exported to the cytoplasm but remained nuclear throughout infection (Fig. 1). Similar results were seen with mutants S16E, S18E, S114E, and S16,18E (data not shown). ICP27 interacts directly with the cellular mRNA export receptor TAP/NXF1 via the LRR in the N terminus of ICP27, and the C-terminal zinc-finger-like region is also required for TAP/NXF1 interaction (8). Interaction with TAP/NXF1 is required for ICP27 export to the cytoplasm (8, 23, 24). The deletion of the LRR in mutant dLeu from residues 6 to 19 confined ICP27 to the nucleus in dLeu-infected cells (Fig. 1). ICP27 is phosphorylated by CK2 at serines 16 and 18 adjacent to the LRR, and Koffa et al. showed that in the presence of DRB, an inhibitor of CK2, ICP27 accumulated in the nucleus (29). We conclude that import of ICP27 is unaffected for the phosphorylation site mutants, but export is impeded.

ICP27 remains associated with splicing speckles throughout infection with phosphorylation site mutants. At early times after infection, ICP27 interacts with splicing factors (6, 48, 50) and colocalizes with splicing speckles (43, 49, 50) in its role as an inhibitor of cellular pre-mRNA splicing. Later in infection, ICP27 disassociates from splicing speckles and begins to shuttle between the nucleus and the cytoplasm (8, 9, 52). Because ICP27 was confined to the nucleus in infections with phosphorylation site mutants, we investigated the localization of mutant ICP27 with splicing speckles. Cells infected with wild-type

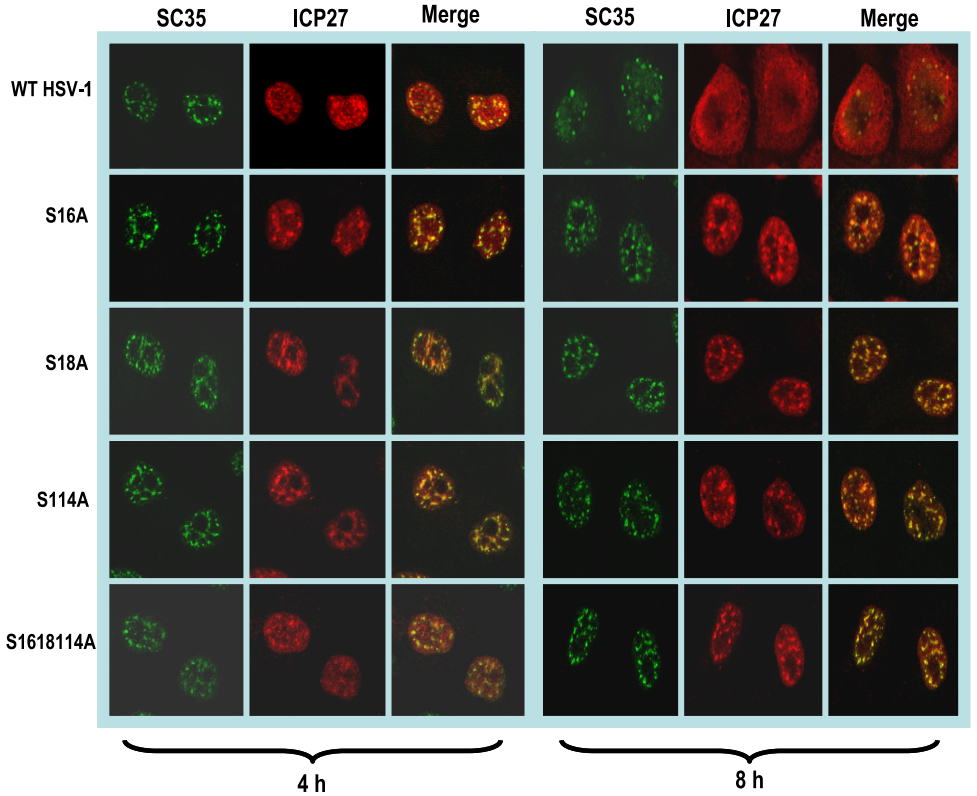

FIG. 2. ICP27 remains associated with splicing speckles throughout infection with phosphorylation site mutants. HeLa cells were infected with HSV-1 KOS, S16A, S18A, S114A, and S16,18,114A at an MOI of 5. At 4 and 8 h after infection, cells were fixed and stained with antibodies to SC35 and ICP27. Images were captured with the LSM 510 confocal microscope. Magnification, ×63.

HSV-1 or mutants S16A, S18A, S114A, and S16,18,114A were stained with monoclonal antibody to SC35, an SR protein splicing factor that marks splicing speckles (16, 50). Wild-type ICP27 was seen to colocalize with SC35 in splicing speckles at 4 h after infection, but by 8 h, ICP27 was diffusely distributed throughout the nucleus and cytoplasm (Fig. 2). In contrast, mutants S16A, S18A, S114A, and S16,18,114A remained associated with SC35 speckles throughout infection (Fig. 2). Similar results were observed with the glutamic acid substitution mutants (data not shown). Therefore, mutant ICP27 is unable to transition from its interaction with splicing factors to undergo the interactions that are required for its activities later in infection, such as export to the cytoplasm (Fig. 1).

ICP27 was not colocalized with Aly/REF during infection with phosphorylation site mutants. Aly/REF is an mRNA export adaptor protein that binds poly(A)$^+$ RNA and interacts directly with TAP/NXF1 to promote export of cellular mRNAs (44, 56). Aly/REF transiently associates with a complex of proteins that is deposited upstream of exon junctions at a late stage of splicing, termed the exon junction complex (11, 30). Aly/REF is recruited to the 5′ ends of transcripts, where it binds to the cap-binding complex protein to form part of the TREX complex, which is required for export of both intronless and spliced mRNAs (5, 36, 55). In uninfected cells, Aly/REF colocalizes with splicing speckles (34, 60). ICP27 colocalizes with Aly/REF at early times after infection and later recruits Aly/REF to viral replication compartments (8, 9). To determine if the phosphorylation site mutant ICP27 can colocalize with Aly/REF, cells were transfected with GFP-Aly/REF and then infected with HSV-1 KOS, S16E, S16,18,114E, or d2-3. Mutant d2-3 has a deletion of amino acids 64 to 108 (31), which includes part of the region of ICP27 required for interaction with Aly/REF (9, 28). At 4 h after infection, wild-type ICP27 colocalized with Aly/REF in splicing speckles (Fig. 3), and by 8 h, ICP27 was shuttling between the nucleus and cytoplasm. There were still nuclear areas of colocalization of ICP27 and Aly/REF at 8 h, and Aly/REF was no longer seen in splicing speckles, but its distribution was in more globular structures that resembled viral replication compartments (Fig. 3), as we reported previously (8). Mutants S16E and S16,18,114E did not show the same colocalization as the wild type with Aly/REF at 4 or 8 h after infection, although both ICP27 and Aly/REF were in speckled-like structures (Fig. 3). Similar results were observed with the alanine substitution mutants (data not shown). This was similar to what we observed with mutant d2-3 (Fig. 3), which cannot interact with Aly/REF (8, 9). These results indicate that the phosphorylation site mutants are unable to colocalize with Aly/REF, and Aly/REF remains in speckled-like structures that are largely distinct from ICP27 speckled structures.

To further address whether phosphorylation site mutant ICP27 can interact with Aly/REF, coimmunoprecipitation experiments were performed on lysates from cells that were mock infected or infected with HSV-1 KOS or S16,18,114A (Fig. 4). Aly/REF was coimmunoprecipitated with wild-type ICP27 and with S16,18,114A mutant ICP27 (Fig. 4) This result indicates

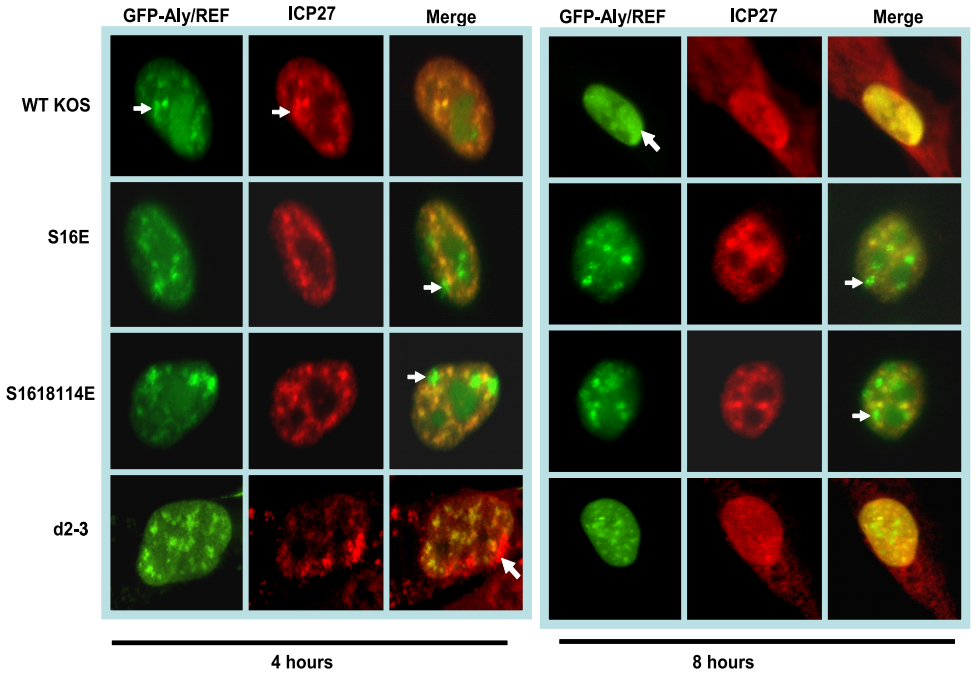

FIG. 3. ICP27 does not colocalize with Aly/REF in infections with glutamic acid substitution mutants. HeLa cells were transfected with pEGFP-Aly/REF and 24 h later were infected with HSV-1 KOS, S16E, S16,18,114E, or d2-3. At 4 and 8 h after infection, cells were fixed, and immunostaining was performed with anti-ICP27 antibody. Green fluorescent protein (GFP) fluorescence was visualized directly. The white arrows point to Aly/REF sites that do not colocalize with ICP27. Images were viewed with Zeiss Axiovert S100 microscope. Magnification, ×100.

that S16,18,114A mutant ICP27 can interact with Aly/REF. However, ICP27 and Aly/REF did not colocalize in infections with the phosphorylation site mutants (Fig. 3), suggesting that the interaction between ICP27 and Aly/REF in the immunoprecipitation experiment may have occurred *in vitro* during the immunoprecipitation procedure. It has been shown that protein complexes and RNA-binding protein complexes may reassociate after cell lysis (35, 40) Therefore, coimmunoprecipitation does not prove that two proteins interact *in vivo*. This appears to be the case for ICP27 and Aly/REF in infections with the phosphorylation site mutants. ICP27 and Aly/REF

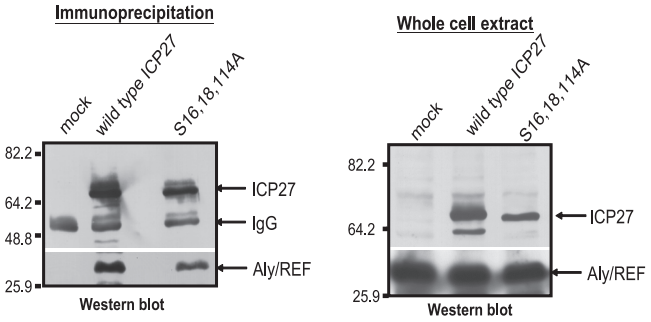

FIG. 4. Aly/REF coimmunoprecipates with mutant ICP27. HeLa cells were mock infected or were infected with HSV-1 KOS or S16,18,114A at an MOI of 5 for 8 h. Immunoprecipitation was performed with anti-ICP27 antibody (left). Western blot analysis was performed with anti-ICP27 antibody and anti-Aly/REF antibody (left). Portions of the whole-cell extracts were fractionated directly on an SDS-polyacrylamide gel, and Western blot analysis was also performed (right). The sizes of the molecular mass markers (in kilodaltons) are indicated on the left.

were localized mostly in different speckled structures within the nuclei of cells infected with phosphorylation site mutants, but *in vitro*, Aly/REF and mutant ICP27 were able to interact (Fig. 4). This result implies that the lack of colocalization between ICP27 and Aly/REF in phosphorylation site mutant-infected cells is not because mutant ICP27 is not capable of interacting with Aly/REF, but rather, mutant ICP27 appears to be stuck in structures that are largely distinct from Aly/REF structures.

ICP27 does not colocalize with TAP/NXF1 in phosphorylation site mutant-infected cells. ICP27 interacts with the cellular mRNA export receptor TAP/NXF1, and ICP27 requires TAP/NXF1 for its export to the cytoplasm (8, 9, 23, 24). Both the N and C termini of ICP27 are required for its interaction with TAP/NXF1 (8). Overexpression of TAP/NXF1 leads to the early export of ICP27 (8, 9) and expression of a TAP/NXF1-dominant negative mutant (8, 9, 24), or reducing TAP/NXF1 levels by small interfering RNA (siRNA) (23) confines ICP27 to the nucleus. The serine residues at positions 16 and 18 are adjacent to the LRR and lie within the N-terminal region of ICP27 required for TAP/NXF1 interaction (8). Further, ICP27 remained in the nucleus in infections with phosphorylation site mutants (Fig. 1). To determine if ICP27 phosphorylation site mutations affect colocalization with TAP/NXF1, immunofluorescence studies were performed. Cells transfected with pEGFP-TAP/NXF1 were infected with HSV-1 KOS, S16E, and S16,18,114E. Wild-type ICP27 was seen to colocalize with TAP/NXF1 at 4 h after infection (Fig. 5), and ICP27 in both the nucleus and the cytoplasm was already detected by 4 h after infection because of overexpression of TAP/NXF1 in cells expressing GFP-TAP/NXF1. Colocalization of ICP27 and

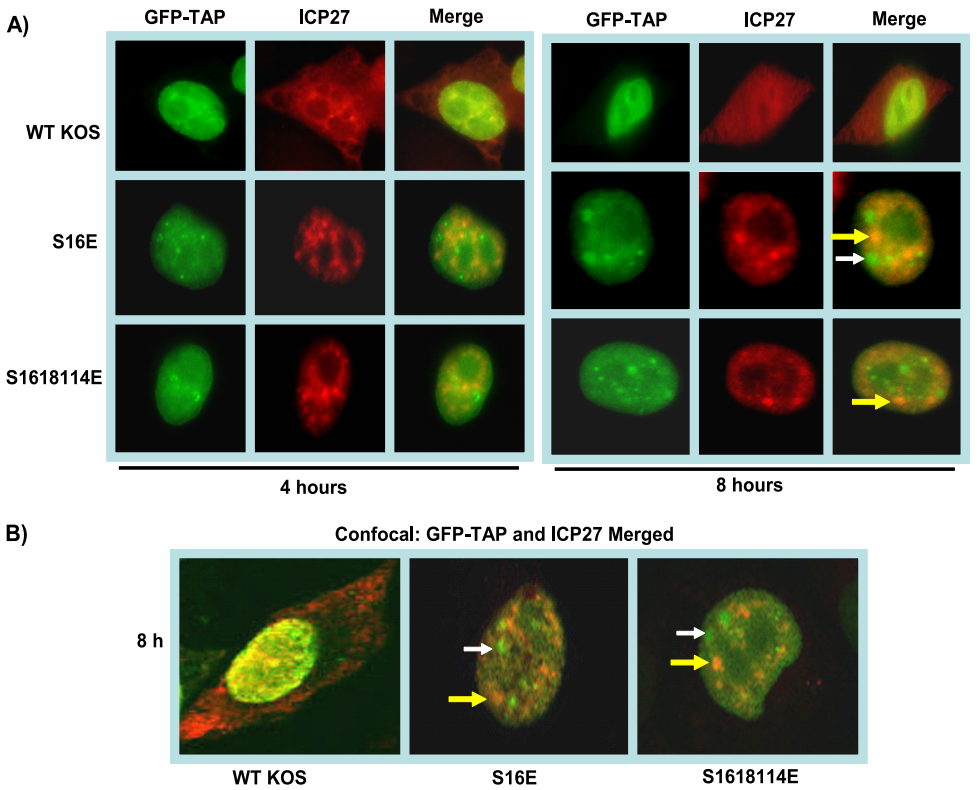

FIG. 5. ICP27 and TAP/NXF1 do not colocalize in infections with phosphorylation site mutants. HeLa cells were transfected with pEGFP-TAP and were subsequently infected with HSV-1 KOS, S16E, or S16,18,114E. Cells were fixed at 4 and 8 h after infection and immunostained with anti-ICP27 antibody. GFP fluorescence was visualized directly. (A) Images were captured with a Zeiss Axiovert S100 microscope. Magnification, ×100. (B) Images were viewed with an LSM 510 confocal microscope. Magnification, ×63. White arrows point to GFP-TAP sites, and yellow arrows mark ICP27 sites in the merged images.

TAP/NXF1 was also visualized in KOS-infected cells at 8 h after infection in both the epifluorescent and confocal merged images (Fig. 5). In contrast, in S16E and S16,18,114E infections, ICP27 remained in the nucleus, and colocalization of ICP27 and TAP/NXF1 was not observed in the cells infected with S16E or S16,18,114E in either the epifluorescent or confocal images (Fig. 5). These results indicate that the mutations introduced at serine 16 and serine 18 impaired the functional interaction of ICP27 with TAP/NXF1. As a result, ICP27 remained in the nucleus throughout infection.

ICP27 alanine substitution and glutamic acid substitution mutants do not complement each other. A surprising finding in this study and in another study describing the construction and characterization of the replication of the phosphorylation site mutants (45) was that all of the mutants behaved similarly. The single, double, and triple substitution mutants had the same phenotypes. Further, the alanine substitution mutants, which were constructed to resemble the unphosphorylated state and the glutamic acid substitutions, which should mimic the negative charge of the phosphorylated state, behaved similarly. This result suggested to us that ICP27 can undergo some interactions, such as interactions with import receptors and splicing factors, regardless of its phosphorylation state, whereas other interactions required ICP27 to be unphosphorylated or phosphorylated. If that were the case, coinfection with alanine substitution mutants and glutamic acid substitution mutants should be more efficient compared to single infections, because both unphosphorylated and phosphorylated forms of ICP27 would be simulated. Therefore, coinfections of the alanine and glutamic acid substitution mutants were performed, and virus yields were compared to those of single infections (Fig. 6). The coinfection experiments were performed three times, and standard deviations are shown (Fig. 6). In essence, there were no significant differences in virus yields in the coinfections compared to single infections, indicating that the alanine and glutamic acid substitution mutants were not able to perform the functions of unphosphorylated and phosphorylated ICP27.

The alanine and glutamic acid substitution mutants show conformational differences compared to unphosphorylated wild-type ICP27. The results of the complementation experiment suggest that the structural changes to a protein that occur as a result of phosphorylation (7, 21, 25) are not being mimicked in the glutamic acid substitution mutants and further that the alanine substitution mutants may have conformational changes compared to unphosphorylated ICP27. To address this, we performed solution structural analysis of the N terminus of ICP27 from amino acids 1 to 160 by NMR spectroscopy. The 160 N-terminal amino acids of ICP27 and triple serine-to-alanine (S16,18,114A) or serine-to-glutamic acid (S16,18,114E) mutants were expressed in Rosetta *E. coli* in minimal medium containing $^{15}NH_4Cl$ to isotopically label the expressed proteins. Protein expression was induced with

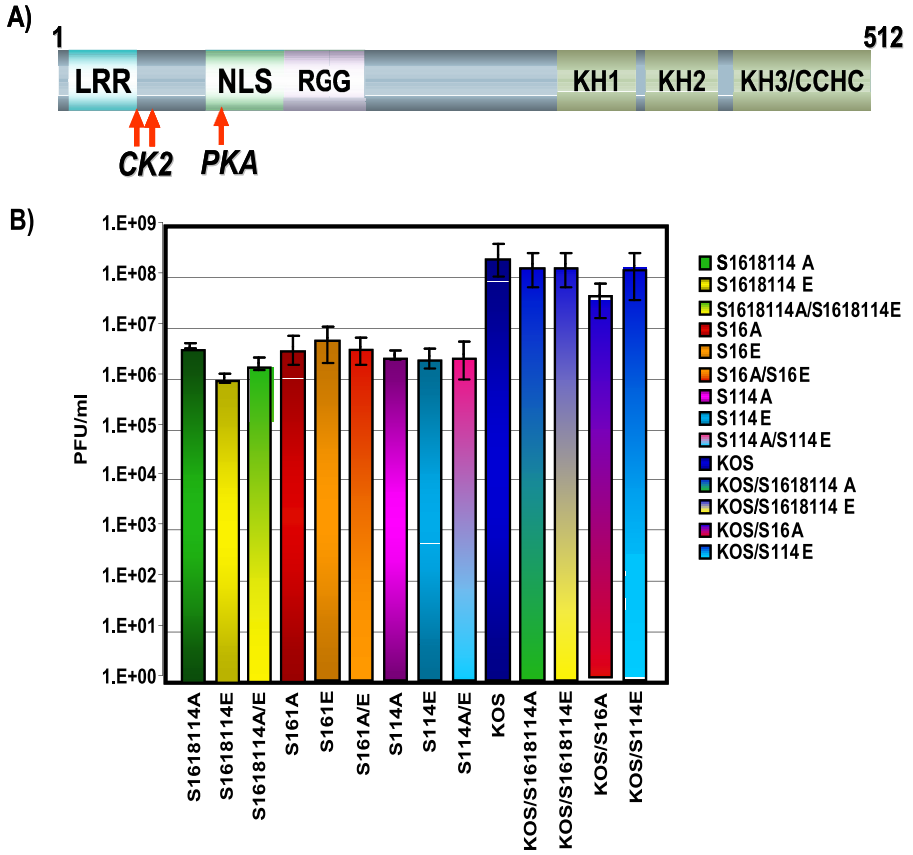

FIG. 6. Alanine and glutamic acid substitution mutants do not complement. (A) Schematic representation of ICP27 illustrating the CK2 and PKA phosphorylation sites denoted by arrows. (B) HeLa cells were infected with the viruses indicated in the figure. Single-virus infections were performed at an MOI of 5. Coinfections were performed at an MOI of 2.5 for each virus. Virus yields were determined by plaque assay on the ICP27 complementing cell line 2-2. Each virus is depicted by a different color, and coinfections are a mix of the two colors for the viruses used in the coinfections.

IPTG, and 6×His-tagged proteins were purified using Ni-NTA agarose under native protein purification conditions. A portion of the elution fractions from the Ni-NTA columns are shown in Fig. 7 for each protein sample used in the NMR analysis.

Two-dimensional NMR was used to analyze the purified proteins. An HSQC experiment was performed on the wild-type and mutant proteins to evaluate the nitrogen and proton spectra of the protein backbone. ^{1}H-^{15}N HSQC correlates the frequency of the amide nitrogen with its directly attached proton, and the spectrum gives a fingerprint of the protein backbone. Each cross peak represents a signal from a single N-H pair. HSQC signals typically distribute based on amino acid type and on local structure; the proton peak position is dominated largely by secondary structure. If a protein is folded, backbone N-H peaks are well dispersed (3).

The wild-type ICP27 HSQC spectra show peaks that were not well dispersed in the proton dimension, and many resonated between 8 and 8.5 ppm (Fig. 8A). HSQC chemical shifts in this range are found typically in proteins with random coil conformations (3), suggesting that the ICP27 N terminus is not well folded. In addition, because each HSQC signal represents one N-H group in the protein, there should be at least one peak per amino acid of the protein. Approximately 70 clearly defined HSQC peaks were observed with the wild-type HSQC spectra, which is less than half of the expected number of 160

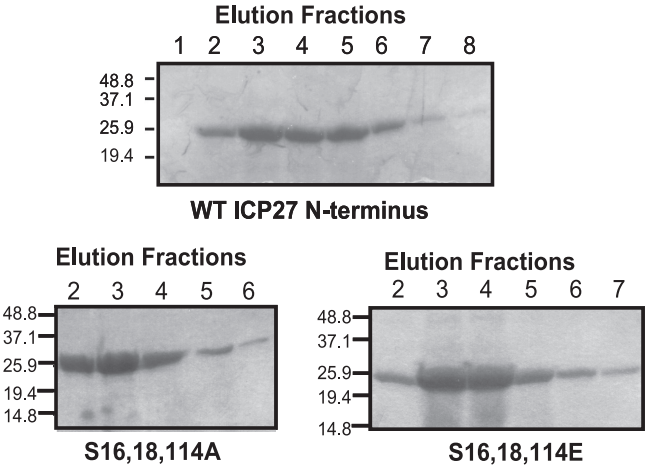

FIG. 7. Expression of ^{15}N-labeled ICP27 N terminus and S16,18,114A and S16,18,114E phosphorylation point mutants. Rosetta *E. coli* cells were transformed with either the pET21b wild-type ICP27 N terminus or phosphorylation point mutant S16,18,114A or S16,18,114E expression plasmids. Cells were grown in Neidhart's minimal media supplemented with $^{15}NH_4Cl$. Protein expression was induced with IPTG, and 6× His-tagged proteins were purified using Ni-NTA agarose under native protein purification conditions. A portion of the elution fractions from the Ni-NTA column was separated on a 10 to 20% Tris gradient gel, and the gel was stained with Coomassie blue.

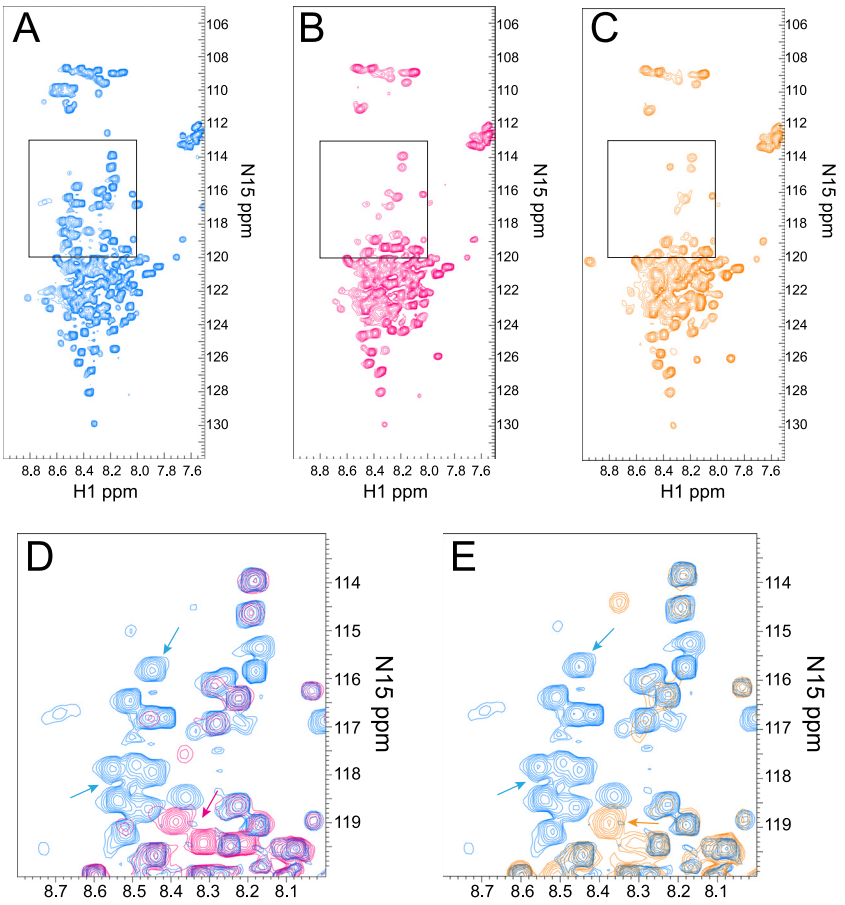

FIG. 8. Alanine and glutamic acid substitution mutations in the ICP27 N terminus show structural changes in two-dimensional (2D) NMR HSQC spectra. (A) The ^{1}H-^{15}N HSQC spectrum for the wild-type ICP27 N terminus. Panels include all peaks detected except for tryptophan. (B) ^{1}H-^{15}N HSQC spectrum for the S16,18,114A mutant. (C) ^{1}H-^{15}N HSQC spectrum for the S16,18,114E mutant. (D) A portion of the full ^{1}H-^{15}N HSQC spectra (boxes in panels A and B) with an overlay of the wild-type ICP27 N terminus (blue) and S16,18,114A mutant (red). Arrows highlight some peaks specifically appearing in either wild-type ^{1}H-^{15}N spectrum (blue arrow) or mutant spectrum (red arrow). (E) A portion of the full ^{1}H-^{15}N HSQC spectra with an overlay of wild-type ICP27 N terminus (blue) and S16,18,114E mutant (orange). Arrows highlight some peaks specifically appearing in either wild-type spectrum (blue arrow) or mutant spectrum (orange arrow).

HSQC peaks (Fig. 8A). There was a high degree of signal overlap in the region between 8.0 and 9.0 ppm in the proton dimension and 120 and 124 ppm in the nitrogen dimension, which prevented the resolution of all 160 HSQC peaks. The lack of peak dispersion and the absence of peaks suggests that the protein does not populate a distinct conformation and is not rigidly folded. Our working model for the structure of the ICP27 N terminus is that it consists of a mix of random coil and molten globule states, suggesting that it is flexible in structure but not completely unfolded.

A similar HSQC analysis was performed on mutants S16,18,1114A (Fig. 8B) and S16,18,114E (Fig. 8C). Significant peak distribution differences were seen with both mutant spectra compared to the wild-type ICP27 N terminus in the region between 120 and 114 in the nitrogen dimension. Peak position is dependent on the chemical environment, and the serine residues that were changed to either alanine or glutamic acid would be expected to shift position. Peaks were absent in the mutant spectra in several regions of the spectra compared to the wild-type spectra (compare Fig. 8A with B and C). Specifically, peaks were absent in the nitrogen axis between 110 and 126 ppm, and several peaks were absent or shifted between 115 and 120 ppm. A closeup of the region between 115 and 120 ^{15}N ppm with the wild-type spectra (Fig. 8D, in blue) and S16,18,114A (Fig. 8D, overlaid in red) shows several wild-type peaks (blue) that were not observed in the spectra for the serine-to alanine-triple mutant (red), and there were peaks seen with this mutant that lack a corresponding wild-type peak. The same was true for mutant S16,18,114E spectra shown in Fig. 8E (orange). We would expect to observe three peaks shifted due to the three serine-to-glutamic acid substitutions, but at least 10 peaks seen with wild-type spectra did not have a corresponding red or orange peak in the mutant spectra, suggesting that these mutations affected a larger portion of the protein than just the three serine residues. Because many peaks were missing in both mutant spectra, this suggests that these mutations have caused the ICP27 N terminus to be even more flexible and unfolded. Interestingly, the same peaks were affected in both mutants, regardless of the change of serine to alanine or glutamic acid. Therefore, these NMR spectra suggest that these serine substitution mutations have an effect on the overall conformation of the N terminus of ICP27.

The alanine and glutamic substitution mutants can still bind RNA. Because both the alanine and glutamic acid substitutions affected the structure of the ICP27 N terminus and because functional interactions of the mutants with Aly/REF (Fig. 3) and TAP/NXF1 (Fig. 5) were impaired, we sought to determine if these mutants were able to undergo another interaction that occurs through the N terminus, namely, RNA binding. ICP27 binds RNA through an RGG box motif from amino acids 138 to 152 (10, 38, 46). Therefore, we assessed the ability of ICP27 mutants S16,18,114A and S16,18,114E to bind RNA by electrophoretic mobility shift assays (EMSA). We showed previously by *in vitro* binding assays that the ICP27 N terminus from amino acid 1 to 160 binds to glycoprotein C (gC) nucleic acid sequences that were derived from a 294-nucleotide sequence that was positive for ICP27 binding in a yeast three-hybrid analysis (10). Overlapping 30-mers from this clone were tested in EMSAs, and it was found that ICP27 bound specifically to sequences that are GC rich and flexible and which do not form stable secondary structures (10). It was further shown in that study that ICP27 bound DNA oligonucleotides as well as RNA oligonucleotides and that the DNA oligonucleotides were more stable (10). Therefore, for this analysis, DNA oligonucleotides were used. The gC sequences are numbered for their positions in the 294-nucleotide yeast three-hybrid clone, which corresponds to nucleotides 96,946 to 97,239 of the coding strand of the KOS HSV-1 gC mRNA. Wild-type ICP27 from amino acids 1 to 160 bound to sequences gC 1-30 and gC 11-40 (Fig. 9A). We showed previously that sequences gC 1-30 and gC 11-40 were shifted well by the ICP27 N terminus (10). Wild-type ICP27 bound poorly to gC 31-60, which we also showed previously (10). Both the alanine and glutamic acid substitution mutants bound gC 1-30 and gC 11-40, and gC 31-60 was not shifted, similar to what was seen with wild-type ICP27 (Fig. 9). This shows that the substitution mutants are binding gC sequences specifically. Therefore, while the S16,18,114A and S16,18,114E mutations affect the structural conformation of the ICP27 N terminus, these mutations do not affect all of the functional interactions that the N terminus of ICP27 engages in because these mutants can still bind gC sequences.

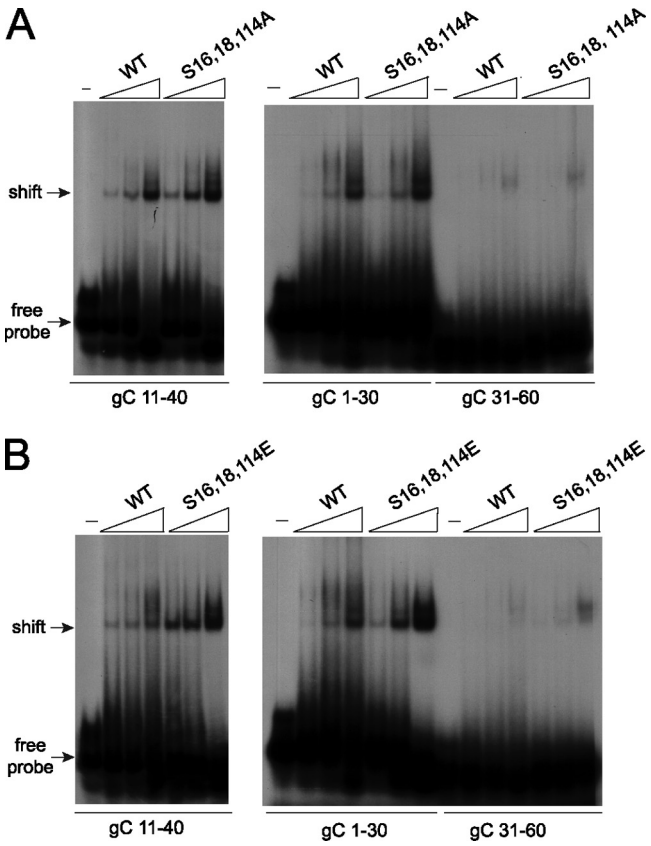

FIG. 9. Alanine and glutamic acid substitution mutants bind HSV-1 gC sequences. (A) Twenty fmol of radiolabeled gC 11–40, gC 1–30, or gC 31–60 30-mer oligonucleotides (see Materials and Methods) were either incubated with no protein (−) or with 2.5 to 62.5 μM wild-type ICP27 N terminus or S16,18,114A N terminus. Samples were fractionated on a prerun acrylamide gel, and dried gels were exposed to film. Arrows indicate the migration of free probe and the shift due to protein binding. (B) Twenty fmol of radiolabeled gC 11–40, gC 1–30, and gC 31–60 30-mer oligonucleotides were either incubated with no protein or 2.5 to 62.5 μM wild-type ICP27 N-terminal protein or S16,18,114E N terminus and were analyzed as described in the legend for panel A.

DISCUSSION

ICP27 performs many different functions during HSV-1 infection, and while several of these functions have been well defined and the mechanisms by which ICP27 mediates its effects elucidated, it is not clear how ICP27 switches between its functional interactions. Posttranslational modifications to proteins can affect protein function. Both arginine methylation and phosphorylation can regulate protein localization, protein-protein interactions, protein-nucleic acid interactions, and protein function (2, 3, 7, 12, 15, 17, 22, 26, 41, 42). ICP27 is modified by both arginine methylation and phosphorylation, and both modifications occur predominantly in the N terminus from amino acids 1 to 160 (38, 45, 53, 58). We have shown that methylation of ICP27 arginine residues 138, 148, and 150 within the RGG box is important for regulating ICP27 export and its interactions with two cellular proteins, Aly/REF and SRPK1 (53, 54).

Unlike arginine methylation, phosphorylation is reversible, and thus, structural changes that are induced by the negatively charged phosphate group can be reversed by dephosphorylation, thus conferring flexibility to phosphorylated proteins to allow switching between different interactions. For example, the yeast shuttling protein Npl3p, which is involved in mRNA export, is phosphorylated on a serine residue in the C-terminal region, and this phosphorylation is important for its import into the nucleus. Dephosphorylation of Npl3p in the nucleus is essential for its interaction with the yeast mRNA export receptor Mex67p and the export of the Mex67p-Npl3/mRNP complex to the cytoplasm (17, 33). Another example of a reversible interaction is that of the fragile-X mental retardation protein, FMRP. FMRP is an RNA-binding protein that is phosphorylated on three serines (42). Phosphorylated FMRP is associated with stalled, untranslating polyribosomes, suggesting that phosphorylated FMRP is involved in translation suppression of mRNAs. Unphosphorylated FMRP has been shown to bind Dicer, whereas phosphorylation disrupts this association, suggesting that phosphorylation of FMRP regu-

lates its association with the microRNA (miRNA) pathway by modulating FMRP's interaction with Dicer (7).

There are many other instances in which phosphorylation on multiple sites can cause protein-protein disassociation or prevent protein-protein association. The inactivation domain of the K^+ channel Kv.4 is regulated by phosphorylation. NMR analysis of the unphosphorylated inactivation domain revealed a compact structure that had a high affinity for its receptor. In contrast, phosphorylation on three serine residues showed a loss of overall stability in the NMR structure, such that regions around the phosphorylated serines were ordered, but residues that were N or C terminal of these sites were disordered, probably from steric and electrostatic repulsion (25). NMR analysis of the ICP27 alanine and glutamic acid substitution mutants showed a degree of disorder higher than that for unphosphorylated ICP27 (Fig. 8). These changes increased the flexibility of ICP27, such that association with Aly/REF (Fig. 3) and TAP/NXF1 (Fig. 5) was impaired. However, unlike phosphorylation, which is reversible, the changes that were induced in the substitution mutants were permanent. The result was that ICP27 became "stuck" in a very early functional association, namely, its interaction with SR splicing proteins in the nucleus, and ICP27 was unable to transition to other functional interactions. Both the alanine and glutamic acid substitutions induced conformation changes in the N terminus, and these changes prevented ICP27 association with several interacting partners. Treatment of cells with the CK2 inhibitor DRB, also trapped ICP27 in the nucleus and prevented it from performing its roles in mRNA export (29). Thus, reversible phosphorylation appears to be important for ICP27 to be able to associate and then disassociate from binding partners so that it can perform its many roles as a multifunctional regulator.

ACKNOWLEDGMENTS

This work was supported by the National Institute of Allergy and Infectious Diseases (NIAID) grants AI61397 and AI21215 to R.M.S.-G. K.A.C.-L. was supported by F32 AI062033 for part of these studies.

REFERENCES

1. **Bachi, A., I. C. Braun, J. P. Rodrigues, N. Pante, K. Ribbeck, C. von Kobbe, U. Kutay, M. Wilm, D. Gorlich, M. Carmo-Fonseca, and E. Izaurralde.** 2000. The C-terminal domain of TAP interacts with the nuclear pore complex and promotes export of specific CTE-bearing RNA substrates. RNA **6:**136–158.
2. **Bedford, M. T., and S. G. Clarke.** 2009. Protein arginine methylation in mammals: who, what and why. Mol. Cell **33:**1–13.
3. **Bedford, M. T., and S. Richard.** 2005. Arginine methylation: an emerging regulator of protein function. Mol. Cell **18:**263–272.
4. **Bontems, S., E. De Valentin, L. Baudoux, B. Rentier, C. Sadzot-Delvaux, and J. Piette.** 2002. Phosphorylation of varicella-zoster virus IE63 protein by casein kinases influences its cellular localization and gene regulation activity. J. Biol. Chem. **277:**21050–21060.
5. **Boyne, J. R., K. J. Colgan, and A. Whitehouse.** 2008. Recruitment of the complete hTREX complex is required for Kaposi's sarcoma-associated herpesvirus intronless mRNA nuclear export and virus replication. PLoS Pathog. **4:**e1000194.
6. **Bryant, H. E., S. Wadd, A. I. Lamond, S. J. Silverstein, and J. B. Clements.** 2001. Herpes simplex virus IE63 (ICP27) protein interacts with spliceosome-associated protein 145 and inhibits splicing prior to the first catalytic step. J. Virol. **75:**4376–4385.
7. **Cheever, A., and S. Ceman.** 2009. Phosphorylation of FMRP inhibits association with Dicer. RNA **15:**362–366.
8. **Chen, I. B., L. Li, L. Silva, and R. M. Sandri-Goldin.** 2005. ICP27 recruits Aly/REF but not TAP/NXF1 to herpes simplex virus type 1 transcription sites although TAP/NXF1 is required for ICP27 export. J. Virol. **79:**3949–3961.
9. **Chen, I. B., K. S. Sciabica, and R. M. Sandri-Goldin.** 2002. ICP27 interacts with the export factor Aly/REF to direct herpes simplex virus 1 intronless RNAs to the TAP export pathway. J. Virol. **76:**12877–12889.
10. **Corbin-Lickfett, K., I. B. Chen, M. J. Cocco, and R. M. Sandri-Goldin.** 2009. The HSV-1 ICP27 RGG box specifically binds flexible, GC-rich sequences but not G-quartet structures. Nucleic Acids Res. **37:**7290–7301. doi:10.1093/nar/gkp.
11. **Custodio, N., C. Carvalho, I. Condado, M. Antoniou, B. J. Blencowe, and M. Carmo-Fonseca.** 2004. In vivo recruitment of exon junction complex proteins to transcription sites in mammalian cell nuclei. RNA **10:**622–633.
12. **Dagher, S. F., and X. D. Fu.** 2001. Evidence for a role of Sky1p-mediated phosphorylation in 3′ splice site recognition involving both Prp8 and Prp17/Slu4. RNA **7:**1284–1297.
13. **Dai-Ju, J. Q., L. Li, L. A. Johnson, and R. M. Sandri-Goldin.** 2006. ICP27 interacts with the C-terminal domain of RNA polymerase II and facilitates its recruitment to herpes simplex virus-1 transcription sites, where it undergoes proteasomal degradation during infection. J. Virol. **80:**3567–3581.
14. **Delaglio, F., S. Grzesiek, G. W. Vuister, G. Zhu, J. Pfeifer, and A. Bax.** 1995. NMRPipe: a multidimensional spectral processing system based on UNIX pipes. J. Biomol. NMR **6:**277–293.
15. **Engel, K., A. Kotyarov, and M. Gaestel.** 1998. Leptomycin B-sensitive nuclear export of MAPKAP kinase 2 is regulated by phosphorylation. EMBO J. **17:**3363–3371.
16. **Fu, X. D., and T. Maniatis.** 1990. Factor required for mammalian spliceosome assembly is localized to discrete regions in the nucleus. Nature **343:**437–441.
17. **Gilbert, W., C. W. Siebel, and C. Guthrie.** 2001. Phosphorylation by Sky1p promotes Np13p shuttling and mRNA dissociation. RNA **7:**302–313.
18. **Hardwicke, M. A., and R. M. Sandri-Goldin.** 1994. The herpes simplex virus regulatory protein ICP27 can cause a decrease in cellular mRNA levels during infection. J. Virol. **68:**4797–4810.
19. **Hardy, W. R., and R. M. Sandri-Goldin.** 1994. Herpes simplex virus inhibits host cell splicing, and regulatory protein ICP27 is required for this effect. J. Virol. **68:**7790–7799.
20. **Hibbard, M. K., and R. M. Sandri-Goldin.** 1995. Arginine-rich regions succeeding the nuclear localization region of the HSV-1 regulatory protein ICP27 are required for efficient nuclear localization and late gene expression. J. Virol. **69:**4656–4667.
21. **Hsu, I., M. Hsu, C. Li, T. Chuang, R. Lin, and W.-Y. Tarn.** 2005. Phosphorylation of Y14 modulates its interaction with proteins involved in mRNA metabolism and influences methylation. J. Biol. Chem. **280:**34507–34512.
22. **Jans, D. A., and S. Hubner.** 1996. Regulation of protein transport to the nucleus: central role of phosphorylation. Physiol. Rev. **76:**651–684.
23. **Johnson, L. A., L. Li, and R. M. Sandri-Goldin.** 2009. The cellular RNA export receptor TAP/NXF1 is required for ICP27-mediated export of herpes simplex virus 1 RNA, whereas, the TREX-complex adaptor protein Aly/REF appears to be dispensable. J. Virol. **83:**6335–6346.
24. **Johnson, L. A., and R. M. Sandri-Goldin.** 2009. Efficient nuclear export of herpes simplex virus 1 transcripts requires both RNA binding by ICP27 and ICP27 interaction with TAP/NXF1. J. Virol. **83:**1184–1192.
25. **Johnson, L. N., and R. J. Lewis.** 2001. Structural basis for control by phosphorylation. Chem. Rev. **101:**2209–2242.
26. **Kaffman, A., N. M. Rank, and E. K. O'Shea.** 1998. Phosphorylation regulates association of the transcription factor Pho4 with its import receptor Pse1/Kap121. Genes Dev. **12:**2673–2683.
27. **Kay, L., P. Keifer, and T. Saarinen.** 1992. Pure absorption gradient enhanced heteronuclear single quantum correlation spectroscopy with improved sensitivity. J. Am. Chem. Soc. **114:**10663–10665.
28. **Koffa, M. D., J. B. Clements, E. Izaurralde, S. Wadd, S. A. Wilson, I. W. Mattaj, and S. Kuersten.** 2001. Herpes simplex virus ICP27 protein provides viral mRNAs with access to the cellular mRNA export pathway. EMBO J. **20:**5769–5778.
29. **Koffa, M. D., J. Kean, G. Zachos, S. A. Rice, and J. B. Clements.** 2003. CK2 protein kinase is stimulated and redistributed by functional herpes simplex virus ICP27 protein. J. Virol. **77:**4315–4325.
30. **Le Hir, H., D. Gatfield, E. Izaurralde, and M. J. Moore.** 2001. The exon-exon junction complex provides a binding platform for factors involved in mRNA export and nonsense-mediated mRNA decay. EMBO J. **20:**4987–4997.
31. **Lengyel, J., C. Guy, V. Leong, S. Borge, and S. A. Rice.** 2002. Mapping of functional regions in the amino-terminal portion of the herpes simplex virus ICP27 regulatory protein: importance of the leucine-rich nuclear export signal and RGG box RNA-binding domain. J. Virol. **76:**11866–11879.
32. **Li, L., L. A. Johnson, J. Q. Dai-Ju, and R. M. Sandri-Goldin.** 2008. Hsc70 focus formation at the periphery of HSV-1 transcription sites requires ICP27. PLoS One **3:**e1491. doi:10.1371/journal.pone.0001491.
33. **Lukasiewicz, R., B. Nolen, J. A. Adams, and G. Ghosh.** 2007. The RGG domain of Npl3 recruits Sky1p through docking interactions. J. Mol. Biol. **367:**249–261.
34. **Luo, M. J., Z. Zhou, K. Magni, C. Christoforides, J. Rappsilber, M. Mann, and R. Reed.** 2001. Pre-mRNA splicing and mRNA export linked by direct interactions between UAP56 and Aly. Nature **413:**644–647.
35. **Mackay, J. P., M. Sunde, J. A. Lowry, M. Crossley, and J. M. Matthews.** 2007. Protein interactions: is seeing believing? Trends Biochem. Sci. **32:**530–531.
36. **Masuda, S., R. Das, H. Cheng, E. Hurt, N. Dorman, and R. Reed.** 2005.

Recruitment of the human TREX complex to mRNA during splicing. Genes Dev. **19:**1512–1517.
37. **Mears, W. E., V. Lam, and S. A. Rice.** 1995. Identification of nuclear and nucleolar localization signals in the herpes simplex virus regulatory protein ICP27. J. Virol. **69:**935–947.
38. **Mears, W. E., and S. A. Rice.** 1996. The RGG box motif of the herpes simplex virus ICP27 protein mediates an RNA-binding activity and determines in vivo methylation. J. Virol. **70:**7445–7453.
39. **Mears, W. E., and S. A. Rice.** 1998. The herpes simplex virus immediate-early protein ICP27 shuttles between the nucleus and cytoplasm. Virology **242:** 128–137.
40. **Mili, S., and J. A. Steitz.** 2004. Evidence for association of RNA-binding proteins after cell lysis: implications for the interpretation of immunoprecipitation analysis. RNA **10:**1692–1694.
41. **Murray, M. V.** 1999. Role of phosphorylation in pre-mRNA splicing. Front. Horm. Res. **25:**83–100.
42. **Patton, E., A. Steeler, and S. Ceman.** 2005. The role of phosphorylation in regulating FMRP function, p. 229–243. *In* Y. J. Sung and R. B. Denman (ed.), The molecular basis of fragile X syndrome. Research Signpost, Kerala, India.
43. **Phelan, A., M. Carmo-Fonseca, J. McLauchlan, A. I. Lamond, and J. B. Clements.** 1993. A herpes simplex virus type 1 immediate-early gene product, IE63, regulates small nuclear ribonucleoprotein distribution. Proc. Natl. Acad. Sci. U. S. A. **90:**9056–9060.
44. **Rodrigues, J. P., M. Rode, D. Gatfield, B. J. Blencowe, M. Carmo-Fonseca, and E. Izaurralde.** 2001. REF proteins mediate the export of spliced and unspliced mRNAs from the nucleus. Proc. Natl. Acad. Sci. U. S. A. **98:**1030–1035.
45. **Rojas, S., K. Corbin-Lickfett, L. Escudero-Paunetto, and R. M. Sandri-Goldin.** 2010. ICP27 phosphorylation site mutants are defective in herpes simplex virus 1 replication and gene expression. J. Virol. **84:**2200–2211.
46. **Sandri-Goldin, R. M.** 1998. ICP27 mediates herpes simplex virus RNA export by shuttling through a leucine-rich nuclear export signal and binding viral intronless RNAs through an RGG motif. Genes Dev. **12:**868–879.
47. **Sandri-Goldin, R. M.** 2008. The many roles of the regulatory protein ICP27 during herpes simplex virus infection. Front. Biosci. **13:**5241–5256.
48. **Sandri-Goldin, R. M., and M. K. Hibbard.** 1996. The herpes simplex virus type 1 regulatory protein ICP27 coimmunoprecipitates with anti-Sm antiserum, and the C terminus appears to be required for this interaction. J. Virol. **70:**108–118.
49. **Sandri-Goldin, R. M., M. K. Hibbard, and M. A. Hardwicke.** 1995. The C-terminal repressor region of HSV-1 ICP27 is required for the redistribution of small nuclear ribonucleoprotein particles and splicing factor SC35; however, these alterations are not sufficient to inhibit host cell splicing. J. Virol. **69:**6063–6076.
50. **Sciabica, K. S., Q. J. Dai, and R. M. Sandri-Goldin.** 2003. ICP27 interacts with SRPK1 to mediate HSV-1 inhibition of pre-mRNA splicing by altering SR protein phosphorylation. EMBO J. **22:**1608–1619.
51. **Smith, I. L., M. A. Hardwicke, and R. M. Sandri-Goldin.** 1992. Evidence that the herpes simplex virus immediate early protein ICP27 acts post-transcriptionally during infection to regulate gene expression. Virology **186:**74–86.
52. **Soliman, T. M., R. M. Sandri-Goldin, and S. J. Silverstein.** 1997. Shuttling of the herpes simplex virus type 1 regulatory protein ICP27 between the nucleus and cytoplasm mediates the expression of late proteins. J. Virol. **71:**9188–9197.
53. **Souki, S. K., P. D. Gershon, and R. M. Sandri-Goldin.** 2009. Arginine methylation of the ICP27 RGG box regulates ICP27 export and is required for efficient herpes simplex virus 1 replication. J. Virol. **83:**5309–5320.
54. **Souki, S. K., and R. M. Sandri-Goldin.** 2009. Arginine methylation of the ICP27 RGG box regulates the functional interactions of ICP27 with SRPK1 and Aly/REF during herpes simplex virus 1 infection. J. Virol. **83:**8970–8975.
55. **Strasser, K., S. Masuda, P. Mason, J. Pfannstiel, M. Oppizzi, S. Rodriguez-Navarro, A. G. Rondon, A. Aguilera, K. Struhl, R. Reed, and E. Hurt.** 2002. TREX is a conserved complex coupling transcription with messenger RNA export. Nature **417:**304–308.
56. **Stutz, F., A. Bachi, T. Doerks, I. C. Braun, B. Seraphin, M. Wilm, P. Bork, and E. Izaurralde.** 2000. REF, an evolutionary conserved family of hnRNP-like proteins, interacts with TAP/Mex67p and participates in mRNA nuclear export. RNA **6:**638–650.
57. **Xie, J., J. Lee, T. L. Kress, K. L. Mowry, and D. L. Black.** 2003. Protein kinase A phosphorylation modulates transport of the polypyrimidine tract-binding protein. Proc. Natl. Acad. Sci. U. S. A. **100:**8776–8781.
58. **Zhi, Y., and R. M. Sandri-Goldin.** 1999. Analysis of the phosphorylation sites of the herpes simplex virus type 1 regulatory protein ICP27. J. Virol. **73:** 3246–3257.
59. **Zhou, C., and D. M. Knipe.** 2002. Association of herpes simplex virus 1 ICP8 and ICP27 with cellular RNA polymerase II holoenzyme. J. Virol. **76:**5893–5904.
60. **Zhou, Z., M. J. Luo, K. Straesser, J. Katahira, E. Hurt, and R. Reed.** 2000. The protein Aly links pre-messenger-RNA splicing to nuclear export in metazoans. Nature **407:**401–405.